 DOI: 10.1002/masy.201000071

Modeling and Multiobjective Optimization of A Fed-Batch Emulsion Copolymerization Process to Control the Resulting Particles Core-Shell Morphology

Brahim Benyahia,[*1,2] *Mohamed Abderrazak Latifi,*[1] *Christian Fonteix,*[1] *Fernand Pla*[1]

Summary: This paper deals with the design and control of the morphology of core-shell nanoparticles elaborated by fed-batch emulsion copolymerization of styrene and butyl-acrylate in the presence of a chain transfer agent (n-dodecyl mercaptan). A mathematical model was elaborated and validated. It consists of a system of differential algebraic equations involving 49 unknown kinetic and thermodynamic parameters, many of them being impossible to be accurately estimated, due to the lack of experimental data. A method based on the sensitivity analysis allowed us to determine a subset of the 21 most influential parameters. The 28 non estimable parameters were taken from the literature. The validated model was then used in a dynamic multiobjective optimization to optimize the best profile of the pre-emulsion feed rate to control (i) the composition and average molar masses of the copolymer, (ii) the instantaneous glass transition temperature, corresponding to a core-shell morphology suited for special end-use properties.

Keywords: core-shell nanoparticles; emulsion copolymerization; modeling; morphology control; multiobjective optimization

Introduction

Emulsion polymerization is an important industrial process used to produce a great variety of polymers for multiple uses (e.g. paints, adhesives, coatings, varnishes ...). Moreover, it has significant advantages over bulk and solution polymerization processes such as heat removal capacity and viscosity control. However, the complexity of emulsion polymerization systems, arising from factors such as their multiphase nature, nonlinear behavior and sensitivity to disturbances, induces more intense difficulties on modeling and makes the development of optimization procedures of emulsion polymerization reactions a very challenging task.

The production of polymers with specified end-use properties is one of the key issues in polymer industry. These properties are strongly governed by both chemical and morphological characteristics, mainly: molecular weight distribution (MWD), polymer microstructure, glass transition temperature (T_g), particles size distribution (PSD) and particles morphology.

In radical polymerizations, molecular weights are commonly controlled using chain transfer agents (CTAs). However, in emulsion polymerization both molecular weights and rate of polymerization are affected by chain transfer agents. The mechanisms of radical desorption and absorption by the particles and, consequently, the particles nucleation and kinetics may be significantly modified.[1–5]

[1] Laboratoire Réactions et Génie des Procédés, UPR 3349 CNRS, Nancy-Université, INPL, 1 rue Grandville B.P. 20451 F-54001 Nancy cedex, France
Fax: +(33) 3 83 17 53 26;
E-mail: brahim.benyahia@ensic.inpl-nancy.fr
[2] Process Systems Engineering Laboratory, Dept. of Chemical Engineering, MIT, 77 Massachusetts Ave, Cambridge MA 02139, USA

On the other hand, the use of multistage emulsion polymerization to produce particles containing multiple polymer phases is widespread throughout coatings, impact plastics and adhesives industries. Such composite particles often improve various end-use properties compared to related single-phase lattices or latex blends. Moreover, the morphology of the resulting particles is generally controlled by a combination of thermodynamic and kinetic factors.[6,7]

The main purpose of this work is to manufacture with high yield, copolymer nanoparticles of a desired morphology, composition and average diameters using a fed-batch emulsion copolymerization of styrene and butyl-acrylate in the presence of n-dodecyl mercaptan, as a chain transfer agent (CTA). This purpose reduces to the simultaneous maximization of the quality and the productivity using multiobjective optimization approach. Optimization problems involving multiple criteria or objective functions are increasingly encountered in chemical industry.[8–11] Because of the competing nature of the objectives (quality, productivity), the solution of such problems is not unique but a set of compromises or non dominated solutions called Pareto's front which depicts trade-offs among the whole objectives.

The key issue of the multiobjective problem is to find the set of best optimal feed rate profiles (time evolution or dynamic) for a multistage copolymerization process which optimizes two objective functions. The first is the minimization of the error between the instantaneous gel transition profile and a designed piecewise constant profile inherent to the desired core-shell morphology. The second deals with the maximization of the final conversion rate.

Prior to the optimization and after the experimental investigation on the effect of the CTA, a mathematical model of the process was elaborated. It consisted of a system of differential algebraic equations, derived from the balance equations (mass, population and moments) and involving 49 unknown kinetic and thermodynamic parameters. Due the structure of the model and a lack of experimental data, many of these parameters were impossible to be accurately estimated. The main limitations to the parameters estimability are their weak effect on the measured outputs and the correlation between these effects. An estimability analysis method based on the calculation of a sensitivity matrix was developed and led to a subset of the 21 most influential parameters. After the parameters identification the model was validated through additional experiments carried out in batch and fed- batch modes.

The multiobjective optimization problem was solved using a genetic algorithm developed for this purpose. The Pareto's front solutions were then ranked according to a decision making approach (Multi-attribute utility theory) in order to select the best compromise to be implemented.

This article first presents a summary of the process model recalled from our recent work including the main assumptions, the balance equations and the parameters identification associated results. The following section describes the multiobjective approach and the results obtained.

Process Model

There are many research contributions on modeling emulsion polymerization processes, starting with the conventional Harkins' model which identifies three stages: nucleation, particles growth and the end of polymerization. The models available in the literature have different degrees of complexity depending upon their scope and application. The most representative have been reviewed.[12,13]

The development of the model is based on several assumptions. In this work, some of these assumptions are made without providing justification, as they are readily accepted and validated in the classical literature. Others which must be given with the necessary explanations are summarized as follows:

- Due to the high surfactant concentration used in this work and the low solubility of styrene, butyl acrylate and n-C12 mercaptan in water, only micellar nucleation is considered,
- Only inhibition and initiation are considered in the water phase,
- The chain transfer agent is subject to diffusional limitations mainly in the droplet-aqueous phase interface,
- The growing particles and the monomer droplets are considered to be monodisperse,
- The reactor is perfectly mixed and isothermal.

Kinetic Scheme

According to the assumptions, the model is based on the following elementary chemical reactions.

In the aqueous phase	
Initiation	$I_2 \xrightarrow{k_d} 2\,R^{\bullet}_{aq}$
Inhibition	$R^{\bullet}_{aq} + Z_{aq} \xrightarrow{k_{zaq}} P + Z^{\bullet}_{aq}$
Nucleation	$R^{\bullet}_{aq} + micelle \xrightarrow{k_N} particle + R^{\bullet}$
Radical absorption	$R^{\bullet}_{aq} + particle \xrightarrow{k_{cp}} particle + R^{\bullet}$
In the organic phase (particles)	
Propagation	$R^{\bullet}_i + M_j \xrightarrow{k_{pij}} R^{\bullet}_j$
Termination by combination	$R^{\bullet}_i + R^{\bullet}_j \xrightarrow{k_{tcij}} P$
Termination by disproportionation	$R^{\bullet}_i + R^{\bullet}_j \xrightarrow{k_{tdij}} 2P$
Inhibition	$R^{\bullet}_i + Z_P \xrightarrow{k_{zpi}} P + Z^{\bullet}_P$
Transfer to monomers	$R^{\bullet}_i + M_j \xrightarrow{k_{trmonij}} P + R^{\bullet}_j$
Transfer to CTA	$R^{\bullet}_i + TA_P \xrightarrow{k_{TApi}} P + TA^{\bullet}_P$
Radical desorption	$R^{\bullet}_i \xrightarrow{k_{desi}} R^{\bullet}_{aq}$

Balance Equations

The material balances are presented in a general form for semi-continuous process using expressions of the reaction rates based on the kinetic scheme presented above. These equations could be easily simplified for the case of a batch process. It must be noted that population balance equations are based on the assumption that the fraction of particles containing j free radicals follows Poisson's law. Thanks to this approach the population balance equations reduces to two differential equations.[1,14]

Material Balance

$$\frac{dV_R}{dt} = Q_f + \sum_{i=1,2}\left(\frac{1}{\rho_{pi}} - \frac{1}{\rho_i}\right) M^i_m \left(R_{pi} + R_{trmi}\right) \tag{1}$$

$$\frac{dM_i}{dt} = -R_{pi} - R_{trmi} + Q_f\left[M_{fi}\right] \tag{2}$$

$$\frac{dM_{Ti}}{dt} = Q_f\left[M_{fi}\right] \tag{3}$$

$$\frac{dI}{dt} = -R_d + Q_f\left[M_{fI}\right] \tag{4}$$

$$\frac{dZ}{dt} = -\left(R_{Zp1} + R_{Zp2}\right) + Q_f\left[M_{fZ}\right] \tag{5}$$

$$\frac{dTA}{dt} = -R_{TAp1} - R_{TAp2} + Q_f\left[M_{fTA}\right] \tag{6}$$

$$\frac{dS}{dt} = Q_{Sf}\left[M_{fS}\right] \tag{7}$$

$$\frac{dN_p}{dt} = R_N \tag{8}$$

$$\frac{dR_1}{dt} = \left(R_N + R_{cp}\right) f_{aq1} - R_{p12} + R_{p21} - R_{trm12} + R_{trm21} - R_{Zp1} - R_{des1} - \left(R_{T11} + R_{T12}\right) \tag{9}$$

$$\frac{dR_2}{dt} = \left(R_N + R_{cp}\right) f_{aq2} - R_{p21} + R_{p12} - R_{trm21} + R_{trm12} - R_{Zp2} - R_{des2} - \left(R_{T22} + R_{T21}\right) \tag{10}$$

$$\frac{d\left(N_P \overline{n} \chi_1\right)}{dt} = \left(R_N + R_{cp}\right) f_{aq1} + R_{trm21} + R_{trm11} + R_{TAp1} - R_{des1} - \left(R_{trm21} + R_{trm11} + R_{p11} + R_{p12} + R_{TAp1} + R_{Zp1}\right)\chi_1 - \left(R_{T11} - R_{T12}\right)\chi_1 \tag{11}$$

$$\frac{d\left(N_P\overline{n}\chi_2\right)}{dt} = \left(R_N + R_{cp}\right) f_{aq2} + R_{trm12} + R_{trm22} + R_{TAp2} - R_{des2} - \left(R_{trm12} + R_{trm22} + R_{p22} + R_{p21} + R_{TAp2} + R_{Zp2}\right)\chi_2 - \left(R_{T11} - R_{T12}\right)\chi_1 \quad (12)$$

Population Balance

$$\frac{d\left(N_p\overline{n}\right)}{dt} = R_N + R_{cp} - \left(R_{Zp} + R_T + R_{des}\right) \quad (13)$$

$$\frac{d\left(N_P\tilde{n}\right)}{dt} = 2\,R_{cp}\overline{n} - \left(\frac{2\tilde{\tilde{n}}}{\tilde{n}} + 1\right) R_T - 2\frac{\tilde{n}}{\overline{n}}\left(R_{Zp} + R_{des}\right) \quad (14)$$

Equations of Moments

$$\frac{d\left(N_p\overline{n}\right)}{dt} = R_N + R_{cp} - \left(R_{Zp} + R_T + R_{des}\right) \quad (15)$$

$$\frac{d\left(N_p\overline{n}\lambda_1\right)}{dt} = R_N + R_{cp} - R_{des} + R_p + \left(R_{trm} + R_{TAp}\right)(1-\lambda_1) - \left(R_{Zp} + R_T\right)\lambda_1 \quad (16)$$

$$\frac{d\left(N_p\overline{n}\lambda_2\right)}{dt} = R_N + R_{cp} - R_{des} + R_p(1 + 2\lambda_2) + \left(R_{trm} + R_{TAp}\right) + (1-\lambda_2) - \left(R_{Zp} + R_T\right)\lambda_2 \quad (17)$$

$$\frac{d\left(N_m\right)}{dt} = R_{Zp} + R_{trm} + R_{TD} + R_{TAp} + \frac{R_{TC}}{2} \quad (18)$$

$$\frac{d\left(N_mL_1\right)}{dt} = \left(R_{Zp} + R_{trm} + R_T + R_{TAp}\right)\lambda_1 \quad (19)$$

$$\frac{d\left(N_mL_2\right)}{dt} = \left(R_{Zp} + R_{trm} + R_{TD} + R_{TAp}\right)\lambda_2 + R_{TC}\left(\lambda_2 + \lambda_1^2\right) \quad (20)$$

Parameters Identification

A first step, prior to the parameters identification is to determine the subset of the potentially estimable parameters through an estimability analysis. Due to the model structure and possible lack of measurements, the estimation of some parameters appeared to be impossible regardless the amount of available data. The main limitations to the parameters estimability are their weak effect on the measured outputs and the correlation between their effects. Moreover, this estimation can lead to significant degradation in the predictive capability of the model. The development of an effective solution to the parameters selection requires establishing a methodology based on the magnitude of the individual effect of each parameter on the measured outputs.[15] This approach has been applied to the 49 parameters of the model leading to a subset of 21 parameters. The aim of the model was to correctly predict simultaneously the global conversion (X_{ove}), the fraction of residual styrene (Fr_2), the number- and weight-average molecular weights (M_n, M_w) and the average particles diameters (d_p). The 21 model parameters were determined by the minimization of the maximum likelihood criterion J based on the logarithm of the sum of square differences between the experimental measurements and the model predictions.[16]

It is noteworthy that the logarithm is introduced in the criteria to give the same importance to the different measured outputs during the parameter identification process.

$$J = \sum_{k=1}^{5} N_k . \ln\left(\sum_{l=1}^{N_k}\left(x_k(t_{kl}) - \widehat{x}_k(t_{kl},\,\theta)\right)^2\right) \quad (21)$$

where N_k is the number of measurements of the variables x_k, t_{kl} is the lth time of measurement of the variable x_k and x_k is the value of x_k predicted by the model using the values θ of the unknown parameters. In this relation, the five variables x_k were: X_{ove}, M_n, M_w , d_p and Fr_2.

Associated Results

The measured data were obtained from several batch runs carried out in a 1-liter jacketed reactor, using 1g of initiator, 60 g of styrene, 60 g of butyl-acrylate and various CTA concentrations and temperatures.[14] Global conversion, residual monomers, M_n and M_w and T_g were determined by gravimetry, GC using a Delsi Nermag DN 200 chromatograph, SEC using a Waters Millipore equipment, DSC using a Pyris 1 Perkin Elmer apparatus, respectively.

Figure 1a shows the time evolution of X_{ove}, for experiments carried out at 60 and 70 °C, each for two different CTA concentrations. As expected, when the temperature is increased the conversion rate is higher. Figure 1b and 1c present the evolution of M_n and M_w versus X_{ove} for the same runs. As expected, both M_n M_w decrease when CTA concentration increases and decrease when the temperature is increased. On the other hand, smaller particles were produced when the temperature increased (Figure 1d). Moreover, due to the difference between the

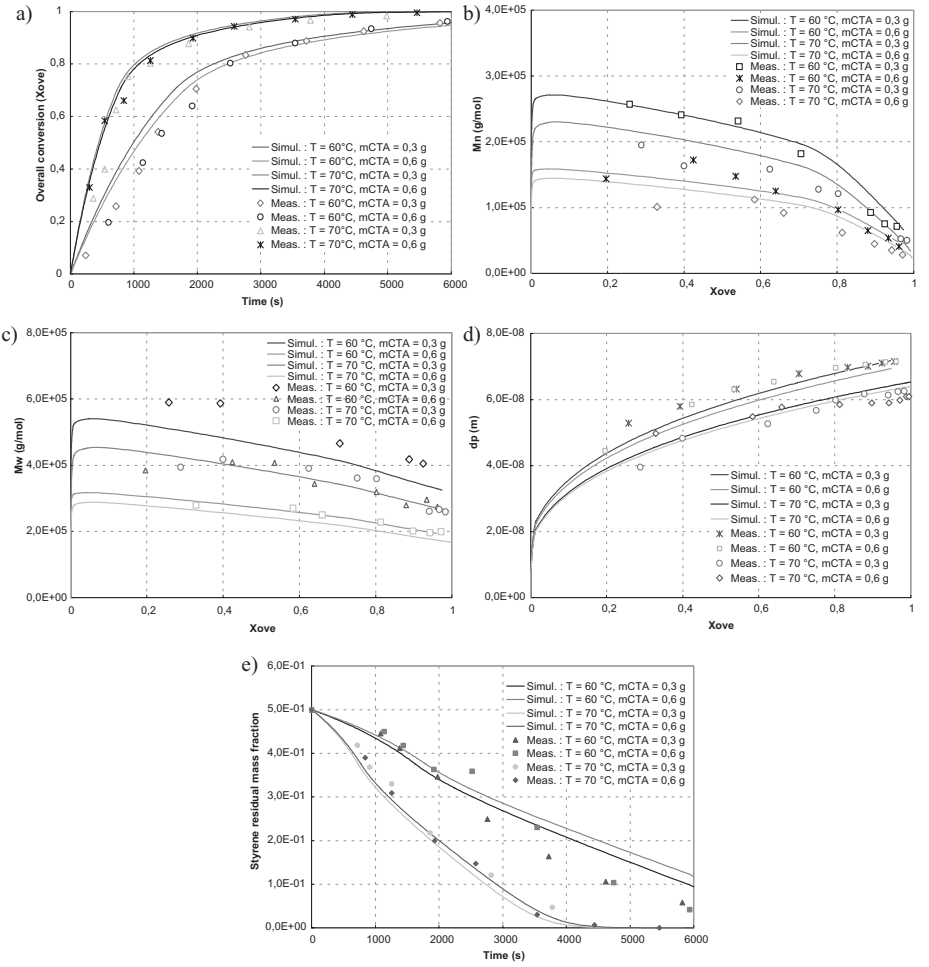

Figure 1.
Effect of the concentration of the CTA and the reaction temperature on: (a) overall conversion. (b) number average molecular weight. (c) weight average molecular weight. (d) particles average diameter. (e) styrene residual mass fraction.

reactivity ratios of each monomer, styrene is consumed faster than butyl-acrylate and the copolymer composition drifts till the total consumption of styrene. Globally the results show an acceptable agreement between simulated and experimental data.

Model Validation

The model was validated using new experimental conditions. The different results obtained for a temperature of 65 °C and a CTA mass of 0.45 g are shown in Figure 2. The results show good agreement. Moreover, the model has been validated under semi batch conditions and the results are not presented here for the sake of brevity.[1]

Multiobjective Optimization

The final objective of this work was to produce core-shell particles having a predesigned glass transition temperature profile that fits film-forming end use properties in the particular case of the paints. These features (the morphology and the T_g profile) endow latex particles with the ability to interpenetrate easily and give the formed film strong properties, particularly a high wet scrub resistance. In the classic approach, core-shell particles are produced using multistage polymerization process (batch or fed batch) where the core is produced during an exclusive emulsion polymerization of the first monomer while the shell is produced exclusively with the second monomer during a second polymerization stage. As a result the core will have different T_g value from the shell (i.e. hard core / soft shell or inverse form). The resulting morphology could be then presented by an instantaneous T_g profile expected to be in the ideal case, piece-wise constant. In our work the desired core-shell morphology is then obtained by tracking a predesigned piece-wise constant T_g profile using a multistage emulsion copolymerization process where monomers copolymerize in each stage (i.e. core and shell) to give more flexibility to the process compared to the classic approach.

Considering that the two monomers used have different reactivity ratios and that the corresponding polymers have different T_g (−54 °C for PBu and 100 °C for PS), the key feature of the optimization problem is to determine the optimal feed rate profiles (feeds and time periods) which

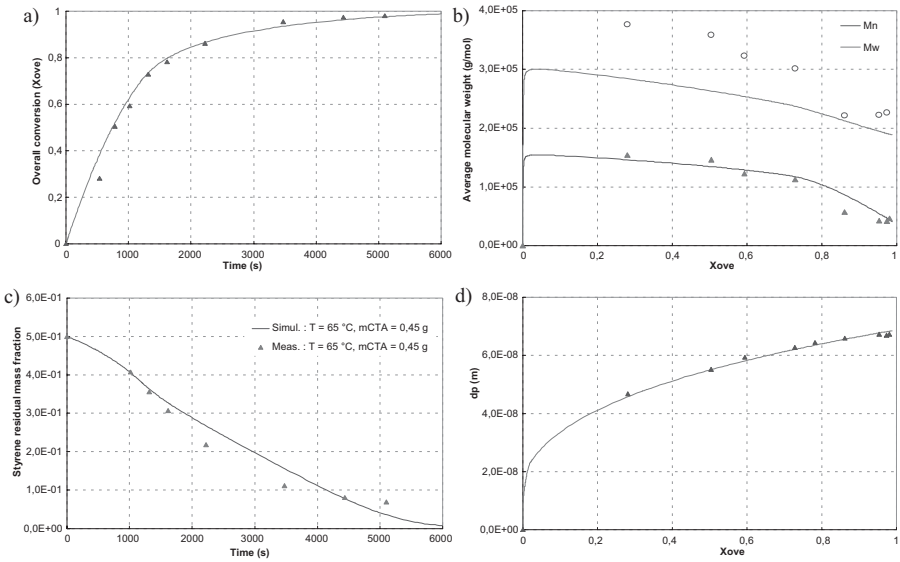

Figure 2.
validation of the process model in batch conditions (a) overall conversion, (b) number and weight average molecular weights, (c) particles average diameter (d) styrene residual mass fraction.

control the polymerization reactions in order to produce particles with the designed glass transition temperature profile associated with the desired morphology.

Two objective functions, f_1 and f_2, given in equations (22), have been selected for the optimization. The first one aims at minimizing the error between the instantaneous glass transition temperature and the desired profile, while the second aims at minimizing the final conversion.

$$
\begin{aligned}
&Min\, f = [f_1, f_2]^T \\
&f_1 = \tfrac{1}{t_{fc}-t_0}\int_{t_0}^{t_{fc}} \left|T_{gi} - T_{g1}\right| dt \\
&\quad + \tfrac{1}{t_{fs}-t_{fc}}\int_{t_{fc}}^{t_{fs}} \left|T_{gi} - T_{g2}\right| dt \\
&f_2 = -X(t_f) \\
&s.t.\ \dot{x} = f(x(t), u(t), p, t);\ x(t=0) = x_0 \\
&\tfrac{1}{t_{fc}-t_0}\int_{t_0}^{t_{fc}} (0.9 - X(t))^2 dt \le \varepsilon^2 \\
&X(t_0) = 0.90 \\
&M_n(t_f) \le 4 \times 10^4 \\
&M_w(t_f) \le 1.5 \times 10^5 \\
&u_{inf} \le u(t) \le u_{sup} \\
&u^T = [\Delta t_1, \Delta t_2, \ldots, \Delta t_n, Q_1, Q_2, \ldots, Q_n]
\end{aligned}
\tag{22}
$$

where T_{gi} is the instantaneous glass transition temperature, T_{g1} the desired glass transition temperature for the core, T_{g2} the desired glass transition temperature for the shell, t_{fc} and t_{fs} the times necessary to obtain the corresponding core and shell respectively, $X(t_f)$ is the conversion at the end of the process and $\boldsymbol{u}$ the control vector (feeds and time periods).

At the first stage of the process (Figure 3), the seeds are produced under batch condition. This stage ends when the overall conversion reaches the value of 0.9. The reactor is then fed with pre-emulsioned monomers and chain transfer agent (CTA). Core stage is designed to be under starving conditions (no droplets are produced and the feed rate is equal to the polymerization rate). Styrene is consumed faster than butyl acrylate due to the difference between there reactivity ratios. As a result, the instantaneous glass temperature will grow to reach the desired value. This stage is operating under a constraint on the overall conversion rate. The shell stage is conducted without required conditions or constraints. Only the objective to reach

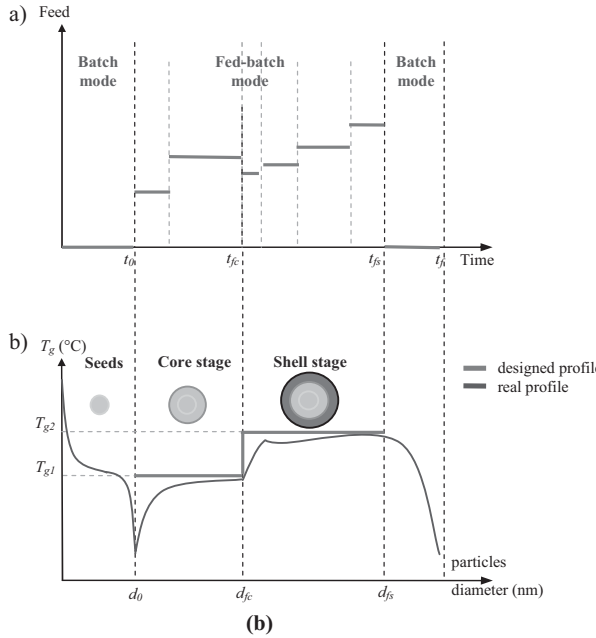

Figure 3.
a. feed rate profile, b. instantaneous glass transition temperature (T_{gi}) profiles.

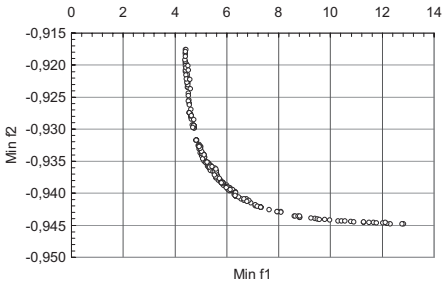

Figure 4.
The Pareto's front of the multiobjective problem (set of non-dominated solutions or best solutions).

the second step of the designed glass temperature profile is kept. Feed rates are more important at this stage to allow the growth of the glass temperature by adding more quantities of styrene. The final stage is operating under batch conditions. Since no styrene is added the residual butyl acrylate is consumed leading to lower glass temperatures. The objective at this stage is to maximize the overall conversion which means maximizing productivity and minimizing residual volatile organic compounds (VOC's).

The feed profiles and the time periods which maximize the conversion at the end of the copolymerization and minimize the difference between the measured and a designed profile of glass transition temperature, were determined by means of a dynamic multi-objective optimization method based on Pareto's approach. The set of non-dominated solutions (Pareto's front) obtained by the use of an evolutionary algorithm[17] is presented in Figure 4.

The best value of the objective functions taken individually are 4.4 (the error between the designed and the resulting profiles) and -0.948 for the criterion related to the final conversion rate.

A decision making tool (Multiattribute utility theory [18]) was then used as a decision making tool to rank Pareto's solutions. The resulting best feed rate and instantaneous glass temperature (T_{gi}) profiles are given in Figure 5. The glass temperature profile obtained (Figure 5b)

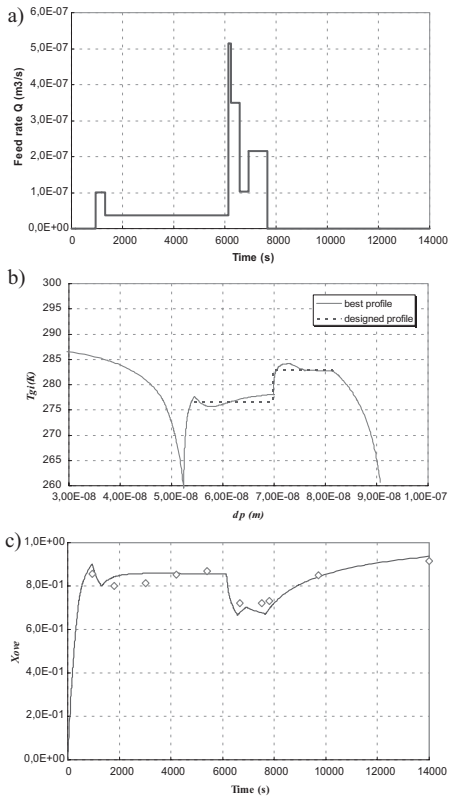

Figure 5.
a. feed rate profile of the best solution, b. instantaneous glass transition temperature profile, c. overall conversion.

corresponds to the designed profile ($T_{g1} = 5\,^{\circ}\mathrm{C}$ and $T_{g2} = 10\,^{\circ}\mathrm{C}$). The first stage (the primary particles formation or seeding) ends with a fall in the glass temperature value. This is quite realistic since butyl acrylate is more consumed when no styrene is added. This phenomenon is also noticed at the end the process.

The overall conversion at the stage of the core formation lies within the limit of the constraint (Figure 5c.). The conversion rate falls during the shell stage as a result of higher feed rates (no constraint on the conversion rate is applied). On the other hand, the last stage (batch process) shows that the overall conversion rate grows to reach the final conversion which is high enough compared to the best solution obtained for the second objective function.

Conclusion

In this work, a dynamic model has been developed and validated for the batch and fed-batch emulsion copolymerization of styrene and butyl-acrylate in the presence of a chain transfer agent (n-dodecyl mercaptan).

After its validation, this model has then been used in a dynamic multiobjective optimization problem designed to determine the optimal feed rate profiles necessary to produce with high yield, copolymer core-shell nanoparticles of a desired composition and average diameters required for particular applications. Thanks to this approach a set of a non dominated solutions (Pareto's front) was obtained and ranked according to a decision making tool. The implementation of the best profile on the real system showed the a good agreement between the objectives and the desired profiles.

[1] B. Benyahia, M. A. Latifi, C. Fonteix, F. Pla, S. Nacef, *Chem. Eng. Sci.* **2010**, *65*, 850.
[2] M. Nomura, Y. Minamino, K. Fujita, M. Harada, *J Polym. Sci.: Polym. Chem.* **1982**, *20*, p. 1261.
[3] M. Nomura, H. Suzuki, H. Tokunaga, K. Fujita, *J Appl. Polym. Sci.* **1994**, *51*, p. 21.
[4] I. Barudio, J. Guillot, G. Fevotte, *J Polym. Sci.* **1998**, *36*, p. 157.
[5] A. Salazar, L. M. Gugliotta, J. R. Vega, G. R. Meira, *Ind. Eng. Chem. Res.* **1998**, *37*, p. 3582.
[6] D. C. Sundberg, Y. G. Durant, *Polym. React. Eng.* **2003**, *11*(3), p. 379.
[7] V. Dimonie, E. Daniels, O. Schaffer, M. El-Aasser, Control of particle morphology, in: P. A. Lovell, M. S. El-Aasser, (Eds.), *Emulsion Polymerization and Emulsion Polymers* John Wiley and Sons, Ltd. London **1997**, p. 293.
[8] C. Fonteix, S. Massebeuf, F. Pla, L. Nandor Kiss, *Eur. J. Oper. Res.* **2004**, *153*, p. 350.
[9] S. Garg, S. K. Gupta, *Macromol. The. Simul. 8*, 46–53. **1999**.
[10] K. Mitra, S. Majundar, S. Raha, *Ind. Eng. Chem.*, *43*, 6055–6063 **2004**.
[11] D. Sakar, S. Rohani, A. Jutan, *AIChE J.*, *53*(5), 1164–1174, **2007**.
[12] J. Gao, A. Penlidis, *Prog. Polym. Sci.* **2002**, *27*, p. 403.
[13] S. C. Thickett, R. G. Gilbert, *Polymer* **2007**, *48*, p. 6965.
[14] B. Benyahia, PhD thesis, National Polytechnic Institute of Lorraine, Nancy-University **2009**.
[15] B. Benyahia, M. A. Latifi, C. Fonteix, F. Pla, *ISCRE 21*, Philadelphia, PA 2010.
[16] E. Walter, L. Pronzato, Com. and Control Eng. Series Springer, London **1997**.
[17] S. Massebeuf, C. Fonteix, S. Hoppe, F. Pla, *J. Appl. Polym. Sci.* **2003**, *87*(14), p. 2383.
[18] S. K. Kim, O. Song, *An. Nucl. Ener.* **2009**, *36*, p. 145.

